

UNCLASSIFIED

AD 296 931

*Reproduced
by the*

**ARMED SERVICES TECHNICAL INFORMATION AGENCY
ARLINGTON HALL STATION
ARLINGTON 12, VIRGINIA**



UNCLASSIFIED

NOTICE: When government or other drawings, specifications or other data are used for any purpose other than in connection with a definitely related government procurement operation, the U. S. Government thereby incurs no responsibility, nor any obligation whatsoever; and the fact that the Government may have formulated, furnished, or in any way supplied the said drawings, specifications, or other data is not to be regarded by implication or otherwise as in any manner licensing the holder or any other person or corporation, or conveying any rights or permission to manufacture, use or sell any patented invention that may in any way be related thereto.

63-2-Y

296 931

MEMORANDUM

RM-3440-PR

JANUARY 1963

INCOHERENT SCATTERING OF RADIO WAVES BY A PLASMA

D. F. DuBois and V. Gilinsky

100-100000

PREPARED FOR:

UNITED STATES AIR FORCE PROJECT RAND

296 931

The **RAND** *Corporation*
SANTA MONICA • CALIFORNIA

MEMORANDUM

RM-3440-PR

JANUARY 1963

**INCOHERENT SCATTERING OF
RADIO WAVES BY A PLASMA**

D. F. DuBois and V. Gilinsky

This research is sponsored by the United States Air Force under Project RAND — Contract No. AF 49(638)-700 — monitored by the Directorate of Development Planning, Deputy Chief of Staff, Research and Technology, Hq USAF. Views or conclusions contained in this Memorandum should not be interpreted as representing the official opinion or policy of the United States Air Force. Permission to quote from or reproduce portions of this Memorandum must be obtained from The RAND Corporation.

The **RAND** *Corporation*

1700 MAIN ST • SANTA MONICA • CALIFORNIA

PREFACE

This report is part of RAND's continuing theoretical study of the properties of high temperature plasmas. The results are of interest for application to the determination of densities and temperatures of high altitude plasmas.

Several installations are under construction to measure the backscatter from powerful radar beams directed vertically upward, and it is hoped that incoherent scattering of electromagnetic waves from a laboratory plasma may be observed.

These experiments and associated theoretical studies will lead to a better understanding of geophysics and electromagnetic wave sciences.

SUMMARY

The incoherent scattering of radio waves from a hot plasma is computed using the diagrammatic techniques of quantum electrodynamics. This method simplifies previously obtained results and permits extensions to include the effects of close collisions.

CONTENTS

PREFACE	111
SUMMARY	v
Section	
I. INTRODUCTION	1
II. FORMULATION	3
III. STANDARD RESULTS BY THE DIAGRAM METHOD	6
IV. THE EFFECT OF COLLISIONS	9
V. DISCUSSION	11
Appendix	
CONNECTION WITH FAMILIAR METHODS	12
REFERENCES	19

I. INTRODUCTION

Several years ago W. E. Gordon⁽¹⁾ suggested that the weak but measurable incoherent scattering of radio waves from electrons at high altitudes would provide information about their density and temperature out to a distance of several thousand kilometers. At frequencies well above the electron plasma frequency $\Omega_p = (4\pi e^2 n/m)^{1/2}$ the ionosphere is essentially transparent. Radio waves are then scattered by charge fluctuations, and the scattered power is proportional to the number of particles. If the particles did not interact among themselves one would obtain for the scattering cross-section N times the familiar individual Doppler-spread cross-section: ⁽¹⁾

$$\frac{d\sigma}{d\omega}(\omega, k) = N r_o^2 \frac{1}{\sqrt{2\pi} k} e^{-\frac{1}{2} \left(\frac{\omega}{k}\right)^2} \frac{1}{2}(1 + \cos^2 k_b \cdot k_a) \quad (1.1)$$

where N is the number of scatterers, $r_o = e^2/m c^2$ is the classical electron radius, $\omega = (\omega_b - \omega_a)/\Omega_p$ is the frequency shift, and $k = (k_b - k_a)/k_D$ is the (vector) change in wave number in units of the Debye wave number $k_D = (4\pi e^2 n/kT)^{1/2}$. The cross-section for backscatter is then $\sigma_{total} = N r_o^2$.

An experiment was performed by K. W. Bowles.⁽²⁾ He observed the incoherent scattering but found that the frequency spread of the returned signal was much narrower than expected, and he proposed⁽³⁾ that the spread of the returned signal was characteristic of the ion velocity and not the electron velocity. Subsequent theoretical investigations by Salpeter,⁽⁴⁾ Dougherty and Farley,⁽⁵⁾ and others⁽⁶⁻⁹⁾ have confirmed this conjecture and have presented a more detailed

picture of the scattered radiation. The shape of the observed signal is determined largely by collective effects.

We shall show here how the standard results are obtained in a simple and transparent way from a diagrammatic theory of many-body electromagnetic interactions.⁽¹⁰⁾ This point of view enables us to include the effects of (close) collisions, which have been neglected by previous authors.

II. FORMULATION

The description of individual electromagnetic processes in terms of Feynman diagrams is at once the clearest, the most elegant, and the most convenient for the purpose of calculation. We shall utilize this method for the problem at hand: the incoherent scattering of photons from a weakly-coupled, high-temperature electron-ion plasma in thermodynamic equilibrium.

The total scattering rate is given by the familiar Golden Rule

$$\Gamma_{\text{total}} = \frac{1}{2} \sum_{e_b, e_a} \int \frac{d^3 k_b}{(2\pi)^3} \sum_2 \sum_1 \rho_1 \frac{1}{2\omega_b 2\omega_a} \left| \langle 2; k_b, e_b | M | 1; k_a, e_a \rangle \right|^2 \quad (2.1)$$

$$(2\pi)^3 \delta^3(P_2 - P_1 + \hbar k_b - \hbar k_a) 2\pi \delta(E_2 - E_1 + \hbar \omega_b - \hbar \omega_a) .$$

The subscripts 1 and 2 refer to the initial and final states of the particles. The subscripts a and b refer to the initial and final states of the radiation (k_a is the initial wave number, e_a is the initial polarization). In Eq. (2.1) we sum over all final states and average over all initial states. The correct average over the initial particles states is obtained by using a suitable Gibbs factor,

$$\rho_1 = e^{\beta\Omega} e^{-\beta(E_1 - \mu N_1)} \quad (2.2)$$

where $\beta^{-1} = kT$, μ is the chemical potential, N_1 is the number of particles in the state 1, and $\exp \beta\Omega$ is the normalizing factor fixed by $\text{Tr} \rho_1 = 1$.

We are, however, interested not in the total transition rate but in the rate to all particle states with the final photon state fixed. We denote this by $\Gamma(k, \omega)$. From Eq. (2.1) one has

$$\Gamma(k, \omega) = \frac{1}{2} \sum_{e_b, e_a} \sum_2 \sum_1 \rho_1 \frac{1}{8\pi^2} \frac{\omega_b}{\omega_a} \left| \langle 2; k_b, e_b | M | 1; k_a, e_a \rangle \right|^2 \quad (2.3)$$

$$(2\pi)^3 \delta^3(P_2 - P_1 + \hbar k) 2\pi \delta(E_2 - E_1 - \hbar\omega) .$$

To obtain the amplitude M we simply draw all possible modes for scattering a photon in state (k_a, e_a) to a state (k_b, e_b) . We can make a number of good approximations. In the non-relativistic limit the diagrams with single photon vertices can be neglected in comparison with diagrams with a double photon vertex. Furthermore, we shall neglect terms of order $\alpha^2 = m/M$, the ratio of the electron and ion masses, so it is not necessary to consider the interaction of the radiation with the ions. In Fig. 1a we show the simplest interaction of interest here. Other possible processes are shown in Figs. 1-3. The braided line represents a screened Coulomb interaction.

The amplitude for any process is readily computed from the corresponding diagram by use of the calculating rules presented in Ref. 10.* For example, the amplitude for the double photon-electron vertex shown in Fig. 1a is given in Ref. 10 to be $(4\pi e^2/m) \hat{e}_b \cdot \hat{e}_a$. The rate for this process is then

*The amplitude may be infinite when the high frequency expansion for that process is not valid. It is then necessary to use a modified perturbation expansion. That is, one must first sum certain classes

$$\Gamma(k, \omega) = \frac{1}{2} \sum_{e_b, e_a} \int \frac{d^3 p_2}{(2\pi)^3} \int \frac{d^3 p_1}{(2\pi)^3} n \left(\frac{2\pi}{m} \right)^{3/2} e^{-\frac{1}{2} p_1^2} \frac{1}{8\pi^2} \frac{\omega_b}{\omega_a} \left| \frac{4\pi e^2}{m} \hat{e}_b \cdot \hat{e}_a \right|^2 \quad (2.4)$$

$$\cdot (2\pi)^3 \delta^3(p_2 - p_1 + \hbar k) 2\pi \delta\left(\frac{1}{2m} p_2^2 - \frac{1}{2m} p_1^2 + \hbar \omega\right).$$

We shall deal only with unpolarized radiation, so we sum and average over the polarizations.

$$\frac{1}{2} \sum_{e_b, e_a} (\hat{e}_b \cdot \hat{e}_a)^2 = \frac{1}{2} (1 + \cos^2 \theta) \quad (2.5)$$

where $k_b \cdot k_a = k_b k_a \cos \theta$. For backscattered radiation one readily obtains the result given in Section 1 for non-interacting particles.

In the following section we shall discuss in detail the many-body processes that produce the central characteristic resonance in the scattered radiation.

of diagrams to remove the divergence at low frequency.

Notice also that the rules for the distribution functions are somewhat different (and simpler) here, since we want only the forward process.

III. STANDARD RESULTS BY THE DIAGRAM METHOD

The scattering due to the process shown in Fig. 1a produces a rather broad line. This is a property of the one-electron pair final state and so is also true of the process shown in Fig. 1b. Since we are interested here mainly in the sharp central line we shall disregard these processes and concentrate on the process shown in Fig. 1c whose ion-pair final state produces a narrow line.

Direct scattering of radiation by an ion, analogous to the electron process in Fig. 1a, also produces a narrow line, but is less important than the process shown in Fig. 1c. There are two reasons for this: (1) the direct photon-ion scattering has an extra factor of $\alpha^4 = (m/M)^2$, and (2) the matrix element for the indirect process (Fig. 1c) has a resonance at the low frequency acoustic mode.

The physical interpretation of Fig. 1c is that the photon (wavy line) is scattered by an electron (the bubble) in the screening cloud which accompanies the ion (heavy line) and interacts with it by means of a screened interaction (braided line). The amplitude for this process is given by (amplitude for double photon-electron vertex) x (amplitude for electron bubble) x (amplitude for screened Coulomb interaction), or in the notation of Ref. 10,

$$\left(1 \frac{\lambda}{c^2} \hat{e}_b \cdot \hat{e}_a\right) (Q_e(k, \omega)) \left(-1 \frac{\lambda}{k^2 + Q(k, \omega)}\right) = \frac{\lambda^2}{c^2} \frac{Q_e}{k^2 + Q} \hat{e}_b \cdot \hat{e}_a \quad (3.1)$$

where $\lambda = k_D^3/n$. The function $Q(k, \omega)$ represents the entire proper polarization part. For the purposes of this section we want Q only

to lowest order, $Q = Q_e^0 + Q_1^0$, the sum of the electron and ion bubbles.

The scattering rate at $\theta = \pi$ is then given by

$$\begin{aligned} \Gamma_a(k, \omega) &= \int \frac{d^3 p_2}{(2\pi)^3} \int \frac{d^3 p_1}{(2\pi)^3} \cdot n \frac{(2\pi)^{3/2}}{\lambda} \alpha^3 e^{-\frac{1}{2} \alpha^2 p_1^2} \frac{1}{8\pi^2} \frac{\omega_b}{\omega_a} \left| \frac{\lambda^2}{c^2} \frac{Q_e}{k^2 + Q} \right|^2 \\ &\quad (2\pi)^3 \delta^3(p_2 - p_1 + \hbar k) 2\pi \delta\left(\frac{1}{2} \alpha^2 p_2^2 - \frac{1}{2} \alpha^2 p_1^2 + \hbar \omega\right) \\ &= n r_o^2 \frac{|Q_e|^2}{|k^2 + Q|^2} \frac{1}{\sqrt{2\pi} \alpha k} e^{-\frac{1}{2} \frac{\omega^2}{\alpha^2 k^2}}. \end{aligned} \quad (3.2)$$

If we take the values of Q_e and Q in the random phase approximation then it is easy to show that this is just the result obtained by previous authors (by rather less direct methods). The subscript a on Γ_a refers to the acoustic mode. The analogous result can be obtained near the plasma resonance by putting $\alpha = 1$ in Eq. (3.2). It should be noted that these results are accurate only near the respective resonances. It is easy to write down a result which is valid over the whole range of frequency but it is more complicated. In Fig. 4 we show several plots of the scattering cross-section in the random phase approximation for several values of k^2 . From Eqs. (6.12) and (6.13) of Ref. 10 we have (with $Z = \omega/\alpha k$)

$$Q_1^0(Z) = 1 - Z e^{-\frac{1}{2} Z^2} \int_0^Z dt e^{\frac{1}{2} t^2} + 1 (\pi/2)^{1/2} Z e^{-\frac{1}{2} Z^2} \quad (3.3)$$

and $Q_e^0 = Q_1^0(\alpha Z)$.

In general, then, we can describe the result as follows. When collective effects are unimportant, that is, when the wave number $k = k_b - k_a$ is large, the scattering is mainly through the mode shown in Fig. 1a. As the wave number transfer k decreases collective effects become increasingly important and processes of the type shown in Figs. 1b and 1c dominate the scattering. The denominator in Eq. (3.2) is the absolute square of the dielectric function of the medium. The scattering is thus enhanced at the resonant frequencies of the medium. There are two such frequencies: the high frequency plasma mode and the low frequency acoustic mode. In the center of the scattered line, where $\omega_b \approx \omega_a$, the scattering is sharply enhanced by the acoustic resonances on each side of ω_a . Since this mode is fairly strongly damped, at least when the electron and ion temperatures are equal, the two resonances run together and the peaks are just barely distinguishable. At about $\omega_b = \omega_a + \Omega_p$ there are sharp resonances corresponding to the electron plasma frequency.

IV. THE EFFECT OF COLLISIONS

To obtain the lowest order effect of (close) collisions we must compute $\Gamma(k, \omega)$ beyond the random phase approximation. In order to correct the shape of the entire spectrum of the scattered radiation it is necessary to have expressions for the collision corrections (or, the conductivity) which are valid for the entire range of frequencies, including very low frequencies. Such expressions are not available in the literature* and the only results which have appeared^(11,12,10) are valid only at high frequencies, that is, when the frequency taken up by the system is greater than some appropriate collision frequency. Nevertheless, one finds that for certain cases the high-frequency formulas apply for a part of the region of interest. They always apply sufficiently far from the center of the line.

We are interested mainly in those processes which broaden the final states in Fig. 1c so that the infinitely sharp energy conserving δ -function in Eq. (3.2) becomes a finite resonance function

$$\frac{1}{\pi} \frac{\hbar \Gamma_p}{(\hbar\omega + \frac{1}{2} \alpha^2 p_2^2 - \frac{1}{2} \alpha^2 p_1^2)^2 + \hbar^2 \Gamma_p^2} \quad (4.1)$$

The width Γ_p is the transport collision frequency for a particle of momentum p . It is the sum of all partial widths for the various collision processes which alter the ion motion.

* One of the authors (D. F. DuBois) has recently obtained such a result for the conductivity of an electron-ion plasma. (To be published.)

We find, therefore, that the important processes are the ones shown in Figs. 2a and 2b. The high-frequency rates are readily computed from the results of Ref. 10.*

To obtain a generally valid result one must in effect consider all iterations of the scattering processes in Fig. 2. At low frequencies the result of this iteration is a Boltzmann-like equation whose solution yields Γ_p .

Other collision processes are shown in Fig. 3. The process shown in Fig. 3a is unimportant because it lacks an ion resonance. Note, however, that both processes are of the same order in the interaction parameter λ because there is a factor λ^{-1} for each closed loop. The process shown in Fig. 3b vanishes in the limit of small frequencies.

*Strictly speaking, the following results are valid only at very high temperatures, say above 10^6 °K, when the Born approximation is valid. At lower temperatures one expects a change only in the argument of the logarithm corresponding to the change in the distance of minimum approach from the thermal deBroglie wave length to e^2/kT .

V. DISCUSSION

A number of problems remain to be solved in order that collision corrections be available for the scattering cross-section for a wide range of parameters. The main problem is to obtain a formula for the conductivity of a plasma which is correct for all frequencies. If this were available it would be possible to extend our results to the center of the line.

For application to scattering from the ionosphere it is important to include the effect of a magnetic field. This depends, of course, on the frequency of the radiation. The neglect of the magnetic field is not a bad approximation at, say, 400 Mc.⁽⁴⁾

There are two interesting extensions of this problem. The first is to permit different temperatures for the electrons and the ions.^(4,9) When the electrons are much hotter than the ions the acoustic mode is very weakly damped and the two peaks in the central line become quite sharp. The other extension⁽⁹⁾ is to allow a relative velocity between the two components. This can further sharpen the resonance, with a very large increase in cross-section, until at some critical velocity the entire system becomes unstable.

It would be interesting to find the effect of collisions on these instabilities.

Appendix

CONNECTION WITH FAMILIAR METHODS

In this appendix we present the problem in an alternate formulation which makes closer contact with more familiar methods. We obtain the well-known result that the scattering cross-section is proportional to the imaginary part of a density correlation function.

The following account is self-contained, but brief. The interested reader will find a more detailed discussion of electromagnetic interactions in plasmas in Ref. 10.

The part of the interaction Hamiltonian which is significant for this problem is

$$H_1(t) = \frac{e^2}{2mc^2} \int d^3x n(x,t) A(x,t) \cdot A(x,t) \quad (A.1)$$

The electromagnetic field is described by the (time-dependent) operator $A(x,t)$ and $n(x,t)$ is the electron density operator.

The amplitude for a transition $1 \rightarrow 2$ is then proportional to

$$\int dt \langle 2; k_b, e_b | H_1(t) | 1; k_a, e_a \rangle$$

$$= \frac{e^2}{2mc^2} \frac{4\pi}{(2\omega_b 2\omega_a)^{1/2}} 2 e_b \cdot e_a \langle 2 | n(0,0) | 1 \rangle \quad (A.2)$$

$$(2\pi)^3 \delta^3(P_2 - P_1 + \hbar k_b - \hbar k_a) 2\pi \delta(E_2 - E_1 + \hbar \omega_b - \hbar \omega_a).$$

One then immediately obtains

$$\Gamma(k, \omega) = r_o^2 \sum_2 \sum_1 \rho_1 \frac{1}{2\pi} \frac{\omega_b}{\omega_a} (e_b \cdot e_a)^2 \left| \langle 2 | n(o, o) | 1 \rangle \right|^2$$

$$(2\pi)^3 \delta^3(p_2 - p_1 + \hbar k) 2\pi \delta(E_2 - E_1 + \hbar \omega) . \quad (A.3)$$

Comparison of Eq. (A.3) with Eq. (4.12) of Ref. 10 shows that the transition rate is proportional to the imaginary part of a density correlation function* $\pi^+(k, \omega)$. We can rewrite Eq. (A.3) in the form:

$$\Gamma(k, \omega) = \frac{r_o^2}{2\pi} \frac{\omega_b}{\omega_a} (1 + \cos^2 \theta) \frac{\text{Im } \pi^+(k, \omega)}{1 - e^{-\hbar \omega}} . \quad (A.4)$$

At high temperatures we can put $1 - e^{-\hbar \omega} \approx \hbar \omega$.

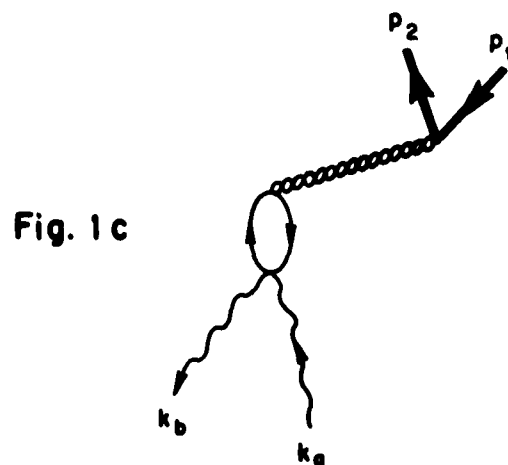
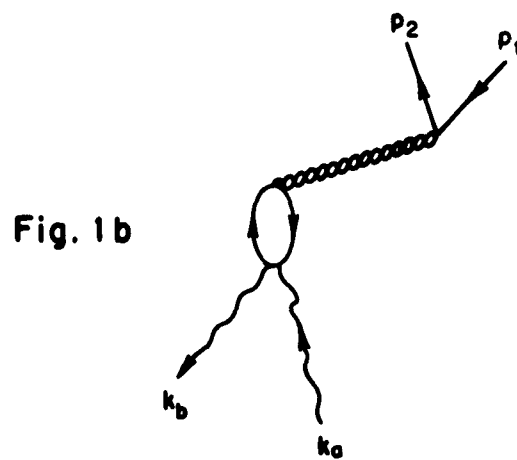
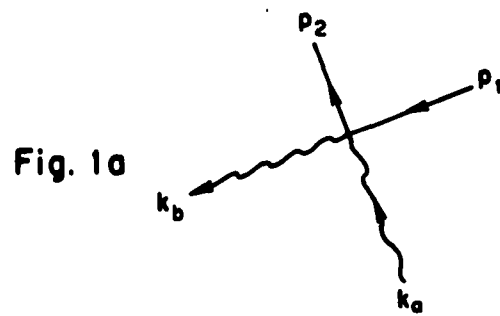
The reader is urged to consult Ref. 10 for a precise definition of $\pi^+(k, \omega)$ and the details of the diagrammatic analysis of this function. The open-diagram techniques lead directly to the results of Section III.

In Fig. 5 we show the diagrammatic description of π , the proper polarization part Q , and the screened interaction V . The correlation function π can be expressed in terms of Q ,

$$4\pi \pi(k, \omega) = Q - Q \frac{1}{1 + k^{-2} Q} Q , \quad (A.5)$$

and, if we drop terms which vanish with $\alpha^2 = m/M$ and put in for Q the expression obtained in the random phase approximation, we immediately get the well-known result for $\Gamma(k, \omega)$ which has been obtained by previous authors.⁽⁴⁻⁹⁾

* The function π^+ differs from the π_{ij}^+ of Ref. 10 only in that the current densities $J_1(o)$ and $J_j(o)$ are replaced by charge densities.



Photon scattering by a free electron (1a), by an electron in the cloud of another electron (1b), and by an electron in the cloud of an ion (1c).

Fig. 2 a

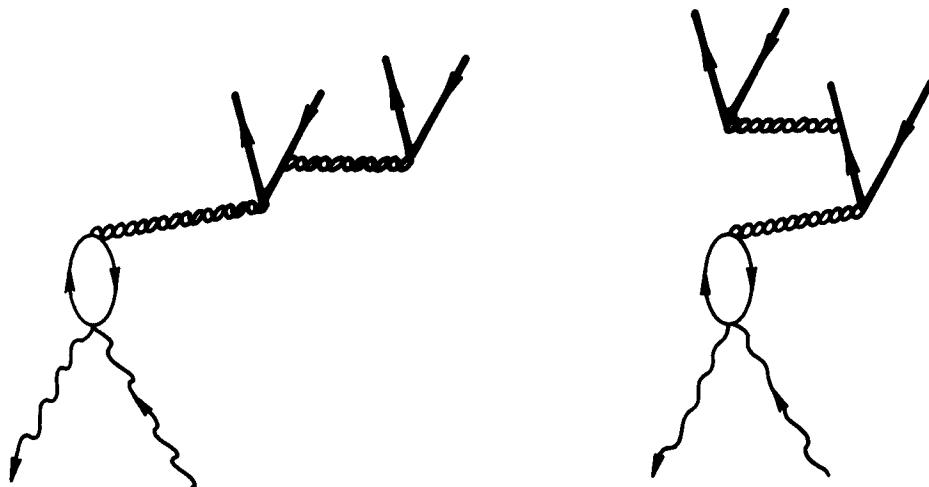
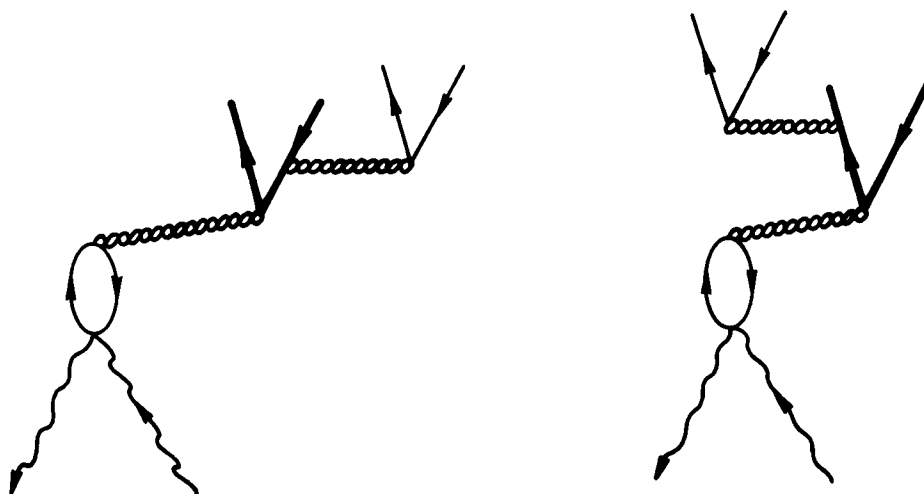


Fig. 2 b



Resonance scattering to a two ion-pair final state (2a) and to a one ion-pair, one electron-pair final state (2b).

Fig. 3a

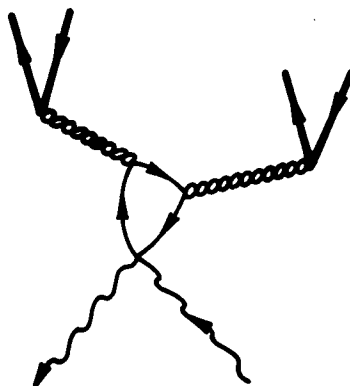
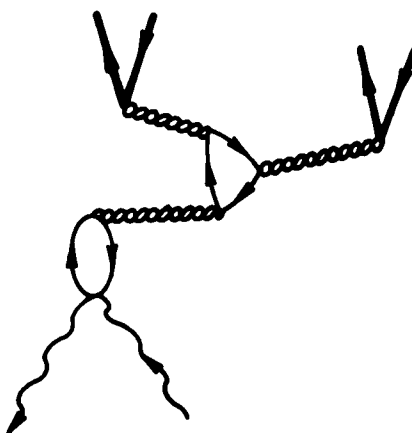


Fig. 3b



Other collision processes

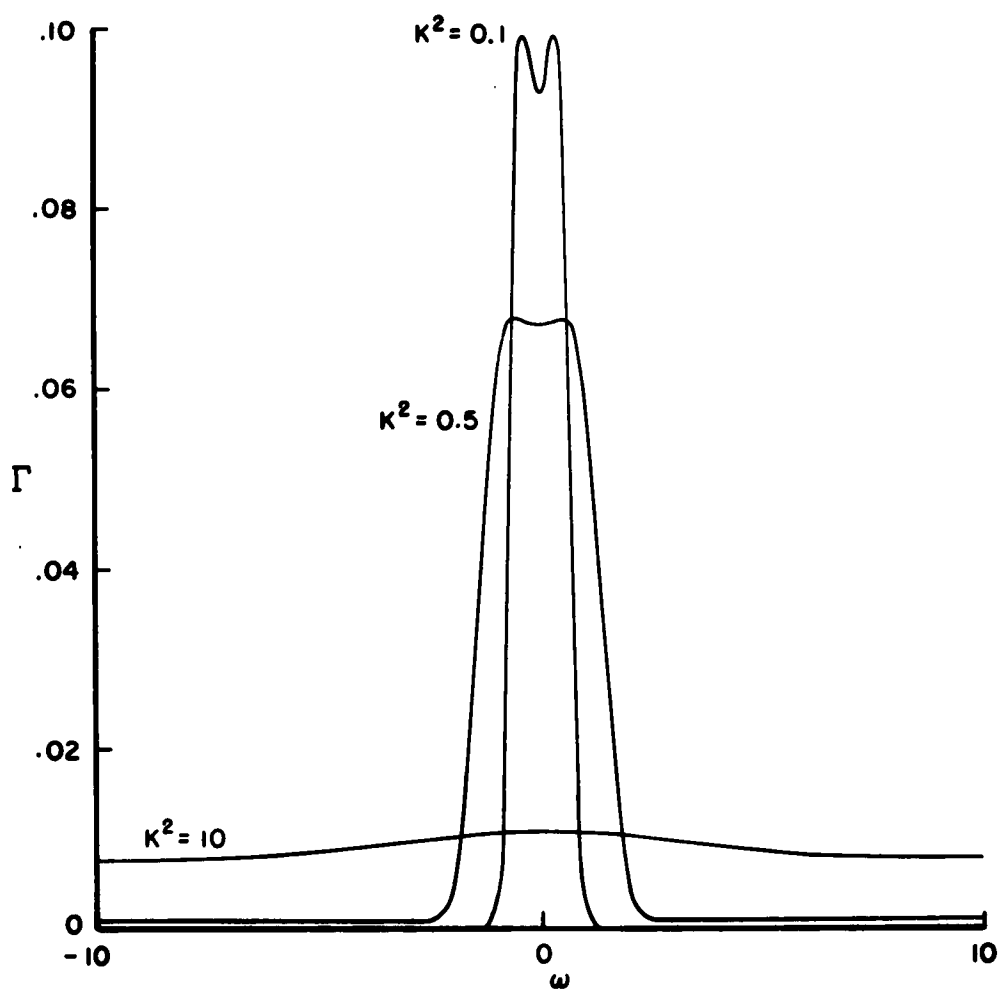


Fig. 4

Scattering line shape in the random phase approximation for several values of κ^2 .

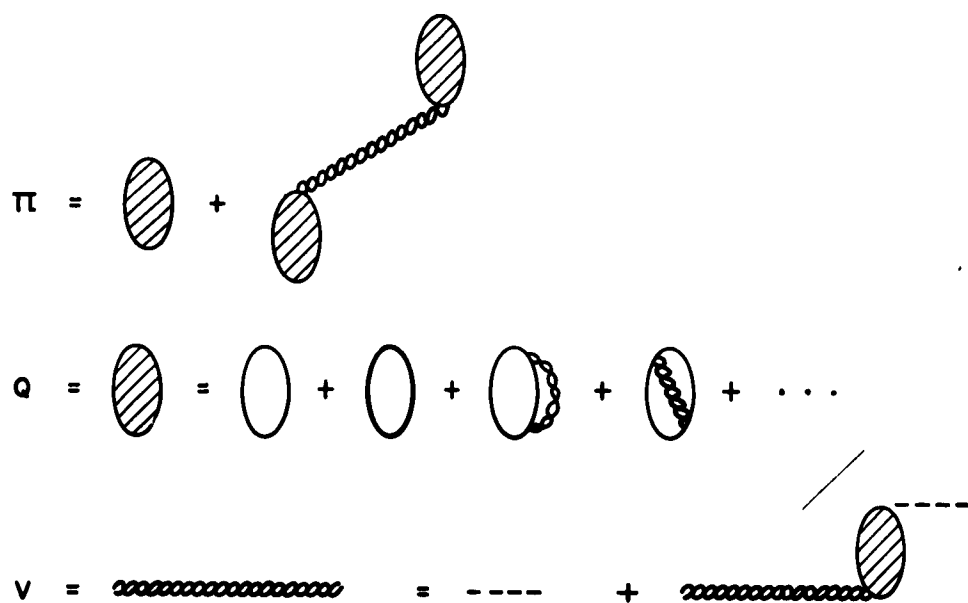


Fig. 5

Diagrammatic description of π , Q , and V .

REFERENCES

1. Gordon, W. E., Proc. Inst. Radio Engrs., Vol. 46, 1958, p. 1824.
2. Bowles, K. L., Phys. Rev. Lett., Vol. 1, 1958, p. 454.
3. Bowles, K. L., National Bureau of Standards Report 6070, Boulder Colorado, 1959.
4. Salpeter, E. E., Phys. Rev., Vol. 120, 1960, p. 1528.
5. Dougherty, J. P., and D. T. Farley, Proc. Roy. Soc. (London), Vol. A259, 1960, p. 79.
6. Renau, J., Jour. Geophys. Res., Vol. 65, 1960, p. 3631.
7. Kahn, F. D., Astrophys. Jour., Vol. 129, 1959, p. 205.
8. Fejer, J. A., Can. Jour. Phys., Vol. 38, 1960, p. 1114.
9. Rosenbluth, M. N., and N. Rostoker, Phys. Fluids, Vol. 5, 1962, p. 776.
10. DuBois, D. F., V. Gilinsky, and M. G. Kivelson, Phys. Rev. (to be published), also as The RAND Corporation RM-3224-AEC, "Propagation of Electromagnetic Waves in Plasmas," August 1962.
The reader should note that the arguments of the logarithms in the expressions for the conductivity in Section VI of RM-3224 are incorrect because diagrams of the type shown in Fig. 3b were overlooked. This introduces a peak near the plasma frequency though the results at high and low frequencies are unchanged.
11. Perel, V. I., and G. M. Eliashberg, Soviet Physics, JETP, Vol. 41, 1961, p. 886.
12. Dawson, J., and C. Oberman, Phys. Fluids, Vol. 5, 1961, p. 517.